Statistical modeling of sequential collision-induced dissociation thresholds

P. B. Armentrout[a)]
Department of Chemistry, University of Utah, Salt Lake City, Utah 84112

(Received 29 March 2007; accepted 25 April 2007; published online 18 June 2007)

Thermochemistry determined from careful analysis of the energy dependence of cross sections for collision-induced dissociation (CID) reactions has primarily come from the primary dissociation channel. Higher order dissociations generally have thresholds measured to be higher than the thermodynamic limit because of the unknown internal and kinetic energy distributions of the primary products. A model that utilizes statistical theories for energy-dependent unimolecular decomposition to estimate these energy distributions is proposed in this paper. This permits a straightforward modeling of the cross sections for both primary and secondary dissociation channels. The model developed here is used to analyze data for $K^+(NH_3)_x$, $x=2-5$, complexes, chosen because the thermochemistry previously determined by threshold CID studies agrees well with values from theory and equilibrium high pressure mass spectrometry. The model is found to reproduce the cross sections with high fidelity and the threshold values for secondary processes are found to be in excellent agreement with literature values. Furthermore, relative thresholds for higher order dissociation processes appear to provide accurate thermodynamic information as well. © *2007 American Institute of Physics*. [DOI: 10.1063/1.2741550]

I. INTRODUCTION

The measurement of thresholds for energy-resolved collision-induced dissociation (TCID) is an accurate method for determining the bond energies of a wide variety of ionized molecules,[1–15] complexes,[16–36] and clusters.[37–43] Such accuracy comes with a price in terms of the careful consideration and control of several experimental factors, as amply illustrated in previous work from our laboratory.[39,44–48] Even for very small systems, it is critical that the energy available to the system be well characterized, which means that internal and kinetic energy distributions of the reactants and the number of collisions between them must be known. As the systems of interest get larger, the lifetime of the dissociation process becomes increasingly important, but it has been shown that statistical theories for unimolecular dissociation[49–51] are generally adequate for accurately accounting for these effects.[52–54] In addition, such statistical methods have provided a straightforward approach to modeling competitive (parallel) dissociation channels from a single complex.[55]

In this paper, this statistical approach is extended to consider sequential reactions, that is, the loss of more than one ligand L from a single complex, reaction (1),

$$M^+L_x + Xe \rightarrow M^+L_{x-1} + L + Xe \rightarrow M^+L_{x-2} + 2L + Xe. \quad (1)$$

The difficulty in analyzing such processes was identified in one of our earliest TCID studies of metal ligand systems.[44,46] Namely, if the cross sections for higher order sequential processes are analyzed using the same methods as those used for the initial dissociation process, the thresholds obtained are generally too high. This observation is illustrated by examining results for the dissociation of the $K^+(NH_3)_x$, $x=1-5$, complexes.[56] This experimental system is used in the present evaluation because the thermochemistry derived from analysis of TCID data of the primary dissociation channels of $x=1-4$ (Ref. 56) agree well with values from equilibrium high pressure mass spectrometry (HPMS) studies[57] as well as *ab initio* calculations at several levels.[56] These bond energies are provided in Table I. If the thresholds for the higher order sequential dissociation channels are analyzed using these same methods, the results listed in Table II are obtained. In all cases, the thresholds obtained are systematically higher than the values expected on the basis of the primary TCID or HPMS results. The shifts get larger as the order of the process increases, being about 0.1 eV for the secondary processes and 0.5 eV for the quaternary process of $K^+(NH_3)_4 \rightarrow K^+ + 4\ NH_3$, and generally increase with the size of the dissociating complex.

The difficulty with analyzing these higher order thresh-

TABLE I. Literature bond dissociation energies at 0 K of $K^+(NH_3)_x$ ($x=1-5$) complexes (in eV).

Reactant ion	Product ion	TCID[a]	HPMS[b]	MP2//B3LYP[c]
$K^+(NH_3)$	K^+	0.82±0.07	0.84±0.09	0.76 (*0.78*)
$K^+(NH_3)_2$	$K^+(NH_3)$	0.71±0.06	0.70±0.09	0.64 (*0.67*)
$K^+(NH_3)_3$	$K^+(NH_3)_2$	0.62±0.05	0.58±0.08	0.56 (*0.59*)
$K^+(NH_3)_4$	$K^+(NH_3)_3$	0.48±0.06	0.51±0.08	0.48 (*0.51*)
$K^+(NH_3)_5$	$K^+(NH_3)_4$	0.32±0.12		0.35 (*0.39*)

[a]Experimental values from Ref. 56 obtained by measuring the primary dissociation thresholds. Uncertainties reported as 2σ.
[b]HPMS values from Ref. 57 converted to 0 K values.
[c]*Ab initio* calculations at the MP2(full)/6-311+G(2d,2p)//B3LYP/6-31G(d) level corrected for zero point energies determined at the B3LYP/6-31G(d) level, and counterpoise corrected. Energies in italics do not include counterpoise corrections for basis set superposition errors.

[a)]Electronic mail: armentrout@chem.utah.edu

TABLE II. Direct fits of thresholds for secondary and higher order dissociation processes at 0 K of $K^+(NH_3)_x$ ($x=2-5$) complexes (in eV). Analysis using Eq. (4). Uncertainties in E_0 reported as 2σ.

Reactant ion	Product ion	σ_0	n	E_0	E_0 (TCID)[a]	E_0 (HPMS)[b]
$K^+(NH_3)_2$	K^+	94.2(44.4)	1.3(0.1)	1.59±0.13	1.53±0.09	1.54±0.13
$K^+(NH_3)_3$	$K^+(NH_3)$	20.9(1.6)	0.6(0.1)	1.46±0.12	1.33±0.08	1.28±0.12
	K^+	2.32(0.43)	1.3(0.2)	2.37±0.24	2.15±0.11	2.12±0.15
$K^+(NH_3)_4$	$K^+(NH_3)_2$	41.4(3.8)	0.6(0.1)	1.27±0.12	1.10±0.08	1.09±0.11
	$K^+(NH_3)$	15.0(1.7)	0.6(0.1)	2.21±0.17	1.81±0.10	1.79±0.14
	K^+	1.8(1.0)	1.4(0.4)	3.16±0.68	2.63±0.12	2.63±0.17
$K^+(NH_3)_5$	$K^+(NH_3)_3$	71.8(5.0)	0.6(0.3)	1.05±0.12	0.80±0.13	

[a]Experimental values calculated using TCID values in Table I.
[b]Experimental values calculated using HPMS values in Table I.

olds is that the initial dissociation process takes away an unknown distribution of energies in translational modes of the initial products, $M^+L_{x-1}+L$, as well as internal modes of the neutral product, L. This leads to a distribution of internal energies in the ionic product that can undergo subsequent dissociations, M^+L_{x-1}, but this distribution is no longer easily defined. Thus, accurate analysis of sequential dissociation products requires making reasonable assumptions about the energy disposal made in the first dissociation, so that the distribution of energies available to the energized molecule in the second dissociation, M^+L_{x-1}, is characterized reasonably well. In this work, reasonable assumptions for statistically behaved systems are outlined and the resulting protocol is tested on the $K^+(NH_3)_x$, $x=2-5$, systems.

II. THEORETICAL TREATMENT

A. Data analysis background

Our approach to reproducing the reaction cross sections for endothermic reactions is to start with the modified line-of-centers model, Eq. (2),

$$\sigma(E) = \sigma_0(E - E_0)^n/E, \tag{2}$$

where σ_0 is an adjustable, energy-independent parameter, n is adjustable parameter that describes the energy deposition efficiency during collision,[58] E is the relative kinetic energy, and E_0 represents the endothermicity at 0 K. To account for the distribution of internal energies of the reactants, this model is modified to include a summation over the rovibrational states i of the reactants with populations g_i, where $\Sigma g_i=1$, yielding Eq. (3),

$$\sigma(E) = \sigma_0 \sum_i g_i(E + E_i - E_0)^n/E. \tag{3}$$

This gives $E+E_i$ as the total energy available to the colliding reactants. Vibrational frequencies and rotational constants used to calculate E_i and g_i are obtained from *ab initio* calculations. The Beyer-Swinehart algorithm[59] is used to evaluate the density of the rovibrational states and the relative populations g_i are calculated for a Maxwell-Boltzmann distribution as appropriate for the particular experimental conditions, in most of our experiments, 300 K. Before final comparison with experimental data, this equation is also convoluted with the distributions of kinetic energies of both the ionic and neutral reagents, as detailed elsewhere.[45]

To include the effect of the dissociation lifetime into our modeling, RRKM theory has previously been incorporated into Eq. (3), as described in detail elsewhere.[54] This transforms Eq. (3) into Eq. (4),

$$\sigma(E) = (n\sigma_0/E)\sum_i g_i \int_{E_0-E_i}^{E} [1 - e^{-k(E^*)\tau}] \times (E - \varepsilon)^{n-1} d\varepsilon. \tag{4}$$

Here, the term in square brackets represent the probability for dissociation (P_D), ε is the energy transferred from translation into internal energy of the ion complex during the collision, τ is the experimental time for dissociation, and E^* is the internal energy of the energized molecule (EM) after the collision, i.e., $E^*=\varepsilon+E_i$. Work has shown that the distribution of deposited energies used in Eq. (4) is consistent with experiment[58] and properly characterized by the parameter n. The term $k(E^*)$ is the unimolecular rate constant for dissociation, as defined by Rice-Ramsperger-Kassel-Marcus (RRKM) theory in Eq. (5),

$$k(E^*,J) = dN^{\dagger}_{\mathrm{vr}}(E^* - E^{\dagger}_R(J) - E_0)/h\rho_{\mathrm{vr}}(E^* - E_R(J)) \tag{5}$$

where the rotational quantum number for the two dimensional (2D) external rotations of the complex is now explicitly introduced. Other terms in Eq. (5) include d, the reaction degeneracy; h, Planck's constant; $N^{\dagger}_{\mathrm{vr}}(E^*-E^{\dagger}_R(J)-E_0)$, the sum of rovibrational states of the transition state (TS) at an energy $E^{\dagger}=E^*-E^{\dagger}_R(J)-E_0$ and $\rho_{\mathrm{vr}}(E^*-E_R(J))$, the density of rovibrational states of the EM at the available energy, $E^*-E_R(J)$. The rotational energies $E^{\dagger}_R(J)$ and $E_R(J)$ are the 2D external rotational energies of the TS and EM, respectively, and J is the rotational quantum number, as discussed more thoroughly in the next section. In the limit that $k(E^*,J)$ is faster than the experimental time available for dissociation of the ions, the term in square brackets in Eq. (4) reduces to unity, and the integration recovers Eq. (3).

B. Treatment of external rotations

A number of possible treatments of the 2D external rotations were discussed by Rodgers *et al.*[54] In all of these, the external 2D rotors of the energized complex are assumed to be adiabatic [hence this energy is unavailable for the dissociation, as explicitly provided in the formulation of Eq. (5)] and centrifugal effects are included as outlined by Waage and Rabinovitch.[60] Thus, the rotational energies at the transition

state differ from those for the energized molecule because as the molecule dissociates, the 2D rotational constant increases. The least biased treatment of the 2D rotations was a statistical assumption that explicitly evaluates the available distribution of J. The final formulation suggested by Rodgers *et al.* was later revised by DeTuri and Ervin[61] who pointed out that the most precise treatment of single channel CID processes was to average the entire dissociation probability over the statistical distribution of rotational quantum numbers, Eq. (6),

$$\langle 1-e^{-k(E^*,J)\tau}\rangle = \frac{\sum_{J=0}^{J_{\max}}[1-e^{-k(E^*,J)\tau}]g_J\rho_{\mathrm{vr}}(E^*-E_R(J))}{\sum_{J=0}^{J_{\max}} g_J\rho_{\mathrm{vr}}(E^*-E_R(J))}, \tag{6}$$

where $g_J=(2J+1)$ is the degeneracy of the 2D rotor, $J_{\max}$ is the maximum value possible for the rotational quantum number determined by energy conservation, $J_{\max}=((1+4E^*/hcB)^{1/2}-1)/2$, and the remaining terms are defined above. The value for $J_{\max}$ comes from the definitions of the rotational energies, namely, $E_R(J)=hcBJ(J+1)$ and $E_R^\dagger(J)=hcB^\dagger J(J+1)$, where B and $B^\dagger$ are the rotational constants of the 2D rotors in the EM and TS, respectively. The expression for P_D in Eq. (6) is substituted for the term in square brackets in Eq. (4), and is now routinely used in our analyses of TCID processes.

If the transition state is tight, then evaluation of $E_R^\dagger(J)$ is straightforward because $B^\dagger$ is well defined. For the more usual case of a loose transition state, $E_R^\dagger(J)$ can be related directly to the height of the centrifugal barrier, $V_{\mathrm{eff}}(r^*)$ above the asymptotic energy of the products. In the case of an ion-induced dipole interaction, this potential is given by $V_{\mathrm{eff}}(r)=\alpha e^2/8\pi\varepsilon_0 r^4+L^2/2\mu r^2$ where α is the polarizability of the neutral product, e is the charge of an electron, ε_0 is the permittivity of vacuum, r is the distance between the products, L is the orbital angular momentum of the products, and μ is the reduced mass of the products. L is equated with the rotational angular momentum, $(J(J+1)\hbar^2)^{1/2}$, which is related to the rotational energy of the EM, $E_R(J)=hcBJ(J+1)$. The height of the barrier is found by setting the derivative of $V_{\mathrm{eff}}(r)$ with respect to r equal to zero, solving for the position of the barrier, r^*, and substituting back into the expression for $V_{\mathrm{eff}}(r)$. This gives the height of the centrifugal barrier as

$$E_R^\dagger(J)=V_{\mathrm{eff}}(r^*)=(\pi\varepsilon_0/2\alpha e^2\mu^2)(\hbar^2 E_R(J)/hcB)^2. \tag{7}$$

This derivation is equivalent to one described by Gilbert and Smith.[49] This variational approach has the distinct advantage of avoiding the problem of needing to guess the geometry of the transition state. This is now determined by the properties of the products, α and μ, and of the EM, $E_R(J)$ and B. To utilize this method, the expression for $E_R^\dagger(J)$ in Eq. (7) is used in evaluating Eqs. (5) and (6), and a statistical distribution of $E_R(J)$ values is explicitly considered.

Extensions of this approach that consider the influence of an ion-dipole long-range potential have also been described.[56] For the $K^+(NH_3)_x$ systems, it was found that the influence of including the dipole on the data analysis changed the thresholds determined by less than 0.02 eV. Hence, the numbers included in Table I were determined using only the ion-induced dipole potential. Likewise, the analysis performed in the present study will not utilize the dipole potential.

C. Sequential dissociations

Conceptually, the application of statistical rate theory to the kinetic energy shifts inherent in a sequential dissociation process is straightforward. This process starts by using Eq. (4) to reproduce the cross section for the sum of the primary and all higher order CID products of reaction (1). Then the probability for further dissociation, $P_{D2}=[1-e^{-k_2(E_2^*,J_2)\tau_2}]$, is included. This partitions the total CID cross section into the cross section for those primary products that do not dissociate (either because they have insufficient energy or because they have insufficient time), $\sigma(M^+L_{x-1})$, and the cross section for those that do, where the latter must equal the cross section for the secondary products, $\sigma(M^+L_{x-2})$. This converts Eq. (4) into

$$\sigma(E,M^+L_{x-1})=(n\sigma_0/E)\sum_i g_i\int_{E_0-E_i}^{E} P_{D1}(1-P_{D2})\times(E-\varepsilon)^{n-1}d\varepsilon, \tag{8a}$$

$$\sigma(E,M^+L_{x-2})=(n\sigma_0/E)\sum_i g_i\int_{E_0-E_i}^{E} P_{D1}P_{D2}(E-\varepsilon)^{n-1}d\varepsilon. \tag{8b}$$

The probability for the second dissociation, P_{D2}, can be calculated in the same fashion as it was for P_{D1} in Eq. (4), namely, $k_2(E_2^*,J_2)$ is calculated using the expression in Eq. (5) for the new energized molecule, M^+L_{x-1} in reaction (1). This requires that the energy available to this EM, E_2^*, is known. As noted above, the energy available to the first EM, M^+L_x in reaction (1), is E_1^*, where the index now differentiates dissociation from the first EM, M^+L_x, from that from the second EM, M^+L_{x-1}. As given above for Eq. (5), the total energy available to the products of the first dissociation, M^+L_{x-1} and L, is $E_1^\dagger=E_1^*-E_{1R}^\dagger(J_1)-E_{0,1}$, where $E_{1R}^\dagger(J_1)$ is the 2D external rotational energy of the initial transition state and $E_{0,1}$ is the threshold energy needed for the first dissociation. Note that this definition of $E_{1R}^\dagger(J_1)$ means that this energy is specifically released into translational motion of the products in order to conserve angular momentum and is therefore unavailable for distribution to the internal energy of the products.

The total energy available to the products, $E_1^\dagger$, can be further partitioned into relative translational energy (T_1) and internal energy of the two products, $E_{1,\mathrm{int}}^\dagger$, i.e., Eq. (9) holds,

$$E_1^\dagger=T_1+E_{1,\mathrm{int}}^\dagger=T_1+E_2^*+E_L, \tag{9}$$

where E_L is the internal energy of the neutral product L of the primary dissociation. In the present work, this partitioning is presumed to be statistically behaved, which provides a robust prediction of the distribution of energies in each of these components. Specifically, the statistical probability of

having products with a particular translational energy, T_1, recognizes that the remainder of the available energy must occupy the internal states of those products. Hence, the density of translational states at T_1 must equal the density of the internal states of the products having the remainder of the energy. This means that the probability of having a specific translational energy T_1 when the available energy is $E_1^\dagger$ is given by Eq. (10),[49,50,62,63]

$$P(T_1;E_1^\dagger) = \rho_{\mathrm{vr}}^\dagger(E_1^\dagger - T_1)d(T_1) \Big/ \int \rho_{\mathrm{vr}}^\dagger(E_1^\dagger - T_1)d(T_1)$$
$$= \rho_{\mathrm{vr}}^\dagger(E_1^\dagger - T_1)d(T_1)/N_{\mathrm{vr}}^\dagger(E_1^\dagger). \quad (10)$$

$N_{\mathrm{vr}}^\dagger(E_1^\dagger)$ can be recognized as the same quantity in the numerator of Eq. (5) for the first dissociation.

It is worth pointing out the relationship of T_1 and $E_{1R}^\dagger(J_1)$ as their sum is the total translational energy of the products, $E_T = T_1 + E_{1R}^\dagger(J_1)$. From the point of view of the reverse association reaction, two species approach one another with a relative translational energy $E_T = \mu v^2/2$. At infinity, they approach one another with an impact parameter b, such that they have an orbital angular momentum $L = \mu v b$. At the point of closest approach, the translational energy can be divided into two terms: one lies perpendicular to the line of centers of the two species and the other is parallel to this line. The former quantity can be identified as the 2D rotational energy of the newly formed complex, $E_{1R}(J_1)$, as noted above, and provides for conservation of angular momentum. The latter term, E_{LOC}, is the energy available for deposition into the internal degrees of freedom of the complex. The relationship between $E_{1R}^\dagger(J_1)$ and $E_{1R}(J_1)$ is given by Eq. (7), which shows that $E_{1R}^\dagger(J_1)$ is less than $E_{1R}(J_1)$. This equation reflects the idea (elucidated by Waage and Rabinovitch[60]) that because the 2D rotational constant of the complex (EM) is generally larger than that of the transition state for dissociation, some energy initially tied up in rotation of the complex is released to other internal degrees of freedom, thereby accelerating the dissociation. Eventually, this difference in rotational energies can also be released to translational energy of the products.

Once the partitioning between the internal and translational energy of the products is accomplished, statistical partitioning of the internal energy between M^+L_{x-1} and L products can be recognized as related to the number of states available, i.e., $N_{\mathrm{vr},2}(E_2^*)$ and $N_{\mathrm{vr},L}(E_L)$, respectively. The probability of having an energy E_2^* in the M^+L_{x-1} product when the total available energy is $E_1^\dagger - T_1$ is calculated using Eq. (11),[49]

$$P(E_2^*;E_1^\dagger - T_1) = \frac{\rho_2(E_2^*)N_L(E_1^\dagger - T_1 - E_2^*)d(E_2^*)}{\int \rho_2(E_2^*)(E_1^\dagger - T_1 - E_2^*)d(E_2^*)}$$
$$= \rho_2(E_2^*)N_L(E_1^* - T_1 - E_2^*)d(E_2^*)/N_{\mathrm{vr}}^\dagger(E_1^\dagger - T_1), \quad (11)$$

where $\rho_2(E_2^*)$ is the density of rovibrational states of M^+L_{x-1} at E_2^* and $N_L(E_1^\dagger - T_1 - E_2^*)$ is the number of rovibrational states of the ligand L at an energy $E_1^\dagger - T_1 - E_2^*$.

Finally, the time available for all dissociation, τ_1, is fixed by the experimental conditions. Thus, the time available for the second dissociation, τ_2, needs to be adjusted by removing the time used in the first dissociation. As the latter is simply $1/k_1(E^*,J_1)$, where $k_1(E^*,J_1)$ is the rate constant for the first dissociation, this is easily accomplished as in Eq. (12),

$$\tau_2 = \tau_1 - 1/k_1(E_1^*,J_1). \quad (12)$$

One can imagine that an exponential distribution of lifetimes should be used to more accurately assess τ_2, but in practice, at the energies needed for the second dissociation to occur, the first dissociation is rapid, such that $\tau_2 = \tau_1$ to a very good approximation.

When all of these steps are combined, the probability for sequential dissociation at an initial excitation energy E_1^* and rotational quantum number J_1 is given by Eq. (13),

$$P_{D2}(E_1^*,J_1) = \int\int P(T_1;E_1^\dagger)P(E_2^*;E_1^\dagger - T_1)\langle 1 - e^{-k_2(E_2^*,J_2)\tau_2}\rangle$$
$$= \frac{\sum_{T_1=0}^{E_1^\dagger}\left[\sum_{E_2^*=0}^{E_1^\dagger - T_1}\langle 1 - e^{-k_2(E_2^*,J_2)\tau_2}\rangle \rho_2(E_2^*)N_L(E_1^\dagger - T_1 - E_2^*) \Big/ \sum_{E_2^*=0}^{E_1^\dagger - T_1}\rho_2(E_2^*)N_L(E_1^\dagger - T_1 - E_2^*)\right]\rho_{\mathrm{vr}}^\dagger(E_1^\dagger - T_1)}{\sum_{T_1=0}^{E_1^\dagger}\rho_{\mathrm{vr}}^\dagger(E_1^\dagger - T_1)}, \quad (13)$$

where the $\langle 1 - e^{-k_2(E_2^*,J_2)\tau_2}\rangle$ term is again given by Eq. (6) which involves an average over a statistical distribution of rotational quantum numbers J_2 for the second dissociation. Note that the integrals in the denominators of Eqs. (10) and (11) have been approximated by a sum in Eq. (13). This is primarily a logistical matter that facilitates more rapid calculation of P_{D2}.

Finally, it is possible that all statistical factors needed to accurately describe the sequential unimolecular dissociation processes are not included in the input parameters. This pos-

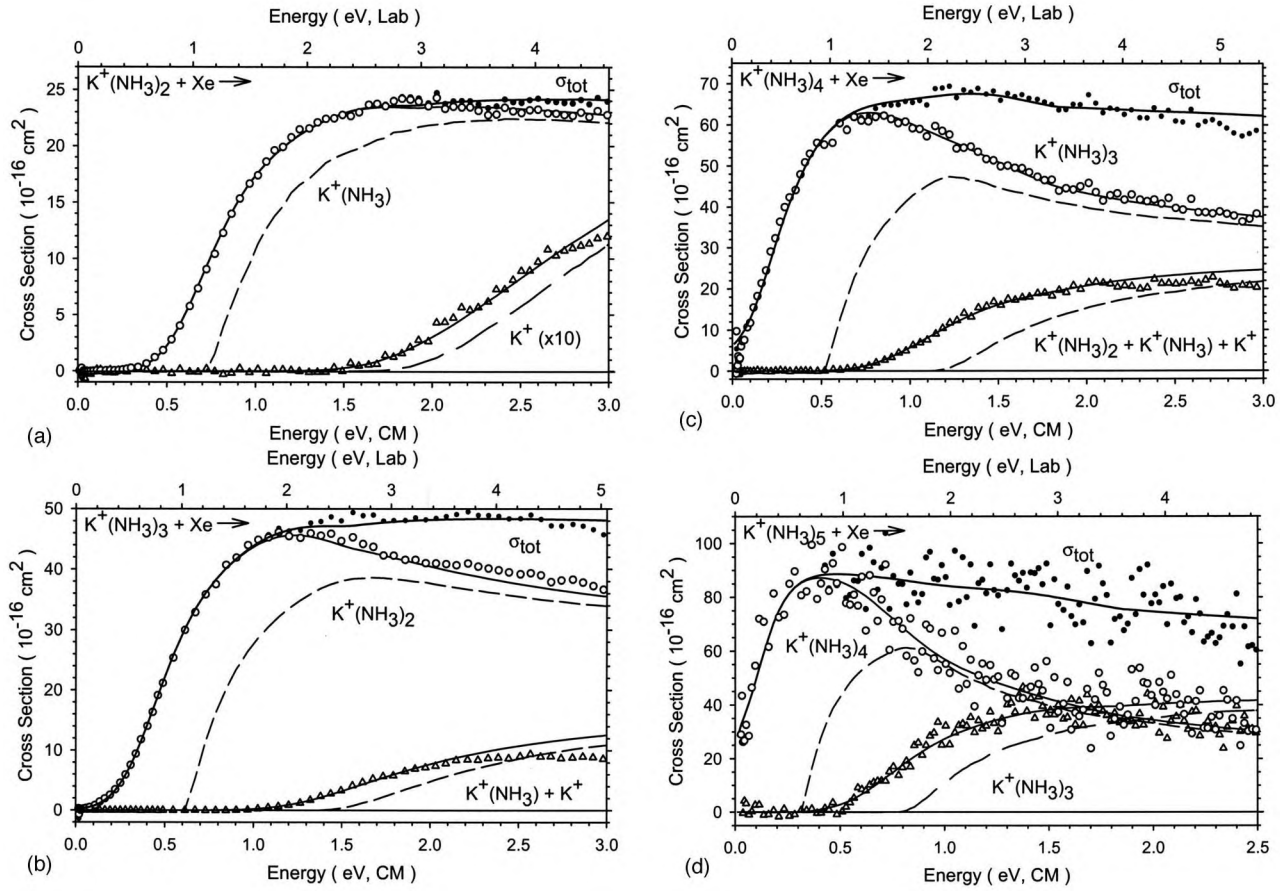

FIG. 1. Zero pressure extrapolated cross sections for collision-induced dissociation of $K^+(NH_3)_x$ where $x=2-5$ (parts a–d, respectively) with Xe in the threshold region as a function of kinetic energy in the center-of-mass frame (lower x axis) and the laboratory frame (upper x axis) taken from Ref. 56. Solid lines show the best fit to the primary and secondary product cross sections using the model of Eq. (8) convoluted over the neutral and ion kinetic and internal energy distributions. Dashed lines show the model cross sections in the absence of experimental kinetic energy broadening for reactions with an internal energy of 0 K. Optimized parameters for the models shown are given in Table III.

sibility is accounted for by multiplying the probability for sequential dissociation, P_{D2}, by an arbitrary scaling factor, f. As shown below, this adjustable parameter is needed to quantitatively describe the sequential dissociation processes. It is hoped that an understanding of this parameter can be gained so that its arbitrariness might be eliminated in future work.

III. APPLICATION AND TESTING

A. Secondary processes

As noted above, the experimental system used for evaluation of this statistical approach to sequential dissociation is $K^+(NH_3)_x$, $x=1-5$. This system exhibits good agreement between the thermochemistry derived from analysis of TCID

TABLE III. Optimized parameters of Eq. (8) for sequential TCID of $K^+(NH_3)_x$ ($x=2-5$) complexes with Xe: Primary and secondary products. Uncertainties in parentheses. Uncertainties in E_0 reported as 2σ. Values in brackets are the relative threshold values.

Reactant ion	Product ion	σ_0	n	E_0 (eV)	E_0 (TCID, eV)[a]
$K^+(NH_3)_2$	$K^+(NH_3)$	38.8(1.1)	0.76(0.05)	0.72(0.08)	0.71(0.06)
	K^+	5.4(0.8)		1.57(0.07)	1.53(0.09)
				[0.85(0.01)]	[0.82(0.07)]
$K^+(NH_3)_3$	$K^+(NH_3)_2$	66.8(0.7)	0.84(0.05)	0.62(0.07)	0.62(0.05)
	$K^+(NH_3)$	28.0(2.1)		1.32(0.07)	1.33(0.08)
				[0.70(0.01)]	[0.71(0.06)]
$K^+(NH_3)_4$	$K^+(NH_3)_3$	82.3(5.0)	0.82(0.10)	0.51(0.09)	0.48(0.06)
	$K^+(NH_3)_2$	42.7(1.3)		1.10(0.08)	1.10(0.08)
				[0.58(0.01)]	[0.62(0.05)]
$K^+(NH_3)_5$	$K^+(NH_3)_4$	90.9(1.5)	0.80(0.20)	0.30(0.14)	0.32(0.12)
	$K^+(NH_3)_3$	66.8(9.0)		0.75(0.15)	0.80(0.13)
				[0.45(0.01)]	[0.48(0.06)]

[a]Experimental values calculated using TCID values in Table I.

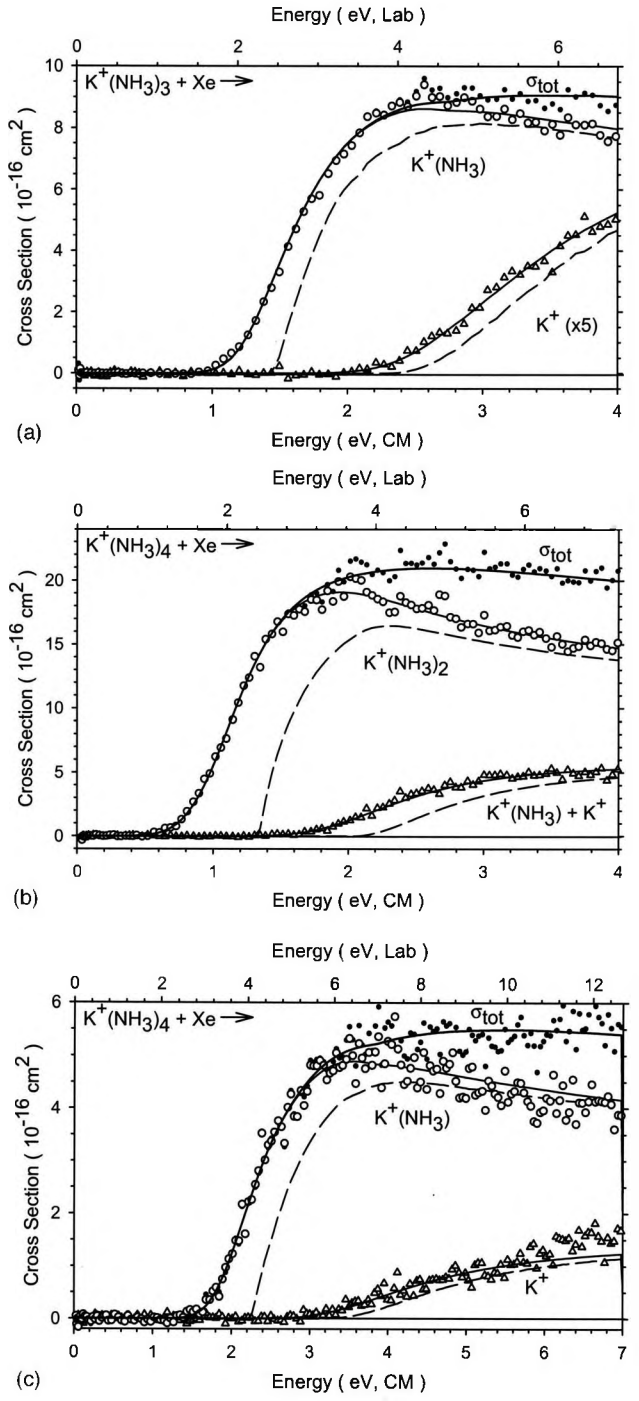

FIG. 2. Zero pressure extrapolated cross sections for collision-induced dissociation of $K^+(NH_3)_x$ where $x=3$ and 4 (parts a–c) with Xe as a function of kinetic energy in the center-of-mass frame (lower x axis) and the laboratory frame (upper x axis) taken from Ref. 56. Solid lines show the best fit to the cross sections for reactions (14) and (15) using the model of Eq. (8) convoluted over the neutral and ion kinetic and internal energy distributions. Dashed lines show the model cross sections in the absence of experimental kinetic energy broadening for reactions with an internal energy of 0 K. Optimized parameters for the models shown are given in Table IV.

data of the primary dissociation channels of $x=1-4$ (Ref. 56) with values from equilibrium high pressure mass spectrometry studies[57] (Table I). Here, both the primary and secondary dissociation channels for collision-induced dissociation of $x=2-5$ are simultaneously reproduced using Eqs. (8). The reproduction of the data for all four complexes is shown in Fig. 1. As can be seen for all four systems, the reproduction of both channels is excellent over extended energy ranges and magnitudes. In all cases, the data near the threshold is reproduced very well down to the noise level.

The optimized parameters used to reproduce these data are given in Table III. The uncertainties in these parameters come from analyses using a range of n values that reproduces the data, variations in the vibrational frequencies of the EM and TS by ±10% and factors of two for the metal-ligand frequencies, variations in τ_1 by factors of two, and the absolute error in the energy scale (0.05 eV, laboratory). Not surprisingly, the agreement between the primary thresholds measured here and those previously measured is good, with differences resulting primarily from slightly different choices of the energy range reproduced. (The biggest differences correspond to cases where the energy range reproduced here is about 1 eV larger than in Ref. 56, which results in slightly lower values of n and slightly higher thresholds.) Some variations might also occur because now there is a more stringent demand to reproduce both the primary and secondary cross sections. Nevertheless, of particular interest here is the comparison of the secondary thresholds obtained from the analysis using Eqs. (8) with those predicted from the sum of the primary thresholds. The agreement is excellent with deviations ranging between 0.00 and 0.05 eV, clearly well within experimental error.

Of additional interest is the comparison of the difference measured here between the primary and secondary thresholds compared to values obtained from primary thresholds (Table III). Because the former are relative measurements, their uncertainties do not include the uncertainty in the absolute energy scale and variations resulting from changes in the vibrational frequencies of the energized molecule and transition states largely cancel as well. Thus the precision of these values is somewhat higher than those of the primary thresholds where these contributions to the uncertainty are included. Excellent agreement is again found between these relative values and the primary TCID thresholds. Overall, the average deviations are 0.02±0.02 eV.

B. Higher order processes

The statistical modeling of the primary and secondary channels is sufficiently successful that it becomes worth exploring whether information about higher order processes might also be obtained. Conceptually, it should be possible to use the same methodology to determine the probability for the tertiary (P_{D3}) and higher order dissociations. However, the computational time required for calculating P_{D2} is already cumbersome for interactive analysis of the data, and that needed for calculating P_{D3} would be prohibitive. Instead, it is possible that the *relative* thresholds of higher order processes may provide useful information. As noted above, the relative thresholds for the primary and secondary processes are determined with higher precision than the absolute thresholds of either process. Although the higher order processes do have thresholds shifted to higher energies (Table II), the statistical analysis of these channels should compensate for this effect between any two subsequent chan-

TABLE IV. Optimized parameters of Eq. (8) for sequential TCID of $K^+(NH_3)_x$ ($x=3$ and 4) complexes with Xe: Higher order products. Uncertainties in parentheses. Uncertainties in E_0 reported as 2σ. Values in brackets are the relative threshold values.

Reactant ion	Product ion	σ_0	n	E_0 (eV)	E_0 (TCID, eV)[a]
$K^+(NH_3)_3$	$K^+(NH_3)$	20.9(1.6)	0.60(0.10)	1.46(0.12)	1.33(0.08)
	K^+	4.86(0.13)		2.24(0.08)	2.15(0.10)
				[0.78(0.05)]	[0.82(0.07)]
$K^+(NH_3)_4$	$K^+(NH_3)_2$	41.4(3.8)	0.64(0.10)	1.27(0.12)	1.10(0.08)
	$K^+(NH_3)$	14.8(0.5)		2.00(0.10)	1.81(0.10)
				[0.73(0.03)]	[0.71(0.06)]
$K^+(NH_3)_4$	$K^+(NH_3)$	15.0(1.7)	0.58(0.08)	2.21(0.17)	1.81(0.10)
	K^+	5.0(0.3)		3.15(0.11)	2.63(0.12)
				[0.94(0.13)]	[0.82(0.07)]

[a]Experimental values calculated using TCID values in Table I.

nels. To test this, the thresholds for the secondary and tertiary reactions (14) were analyzed for $x=3$ and 4,

$$K^+(NH_3)_x + Xe \rightarrow K^+(NH_3)_{x-2} + 2NH_3 + Xe \rightarrow K^+(NH_3)_{x-3} + 3NH_3 + Xe \quad (14)$$

as well as the still higher order process, reaction (15),

$$K^+(NH_3)_4 + Xe \rightarrow K^+(NH_3) + 3NH_3 + Xe \rightarrow K^+ + 4NH_3 + Xe. \quad (15)$$

The results are shown in Fig. 2 where again the reproduction of both channels of the data can be seen to be excellent over extended energy and magnitude ranges. The optimized parameters used are given in Table IV. As expected, the absolute thresholds of both channels are shifted to higher energies than those predicted using the literature thermochemistry in all three systems. However, the relative thresholds for reactions (14) are found to be in good agreement with the expected values, certainly within the experimental uncertainty. In the case of the quaternary reaction (15), the relative threshold is somewhat high although still within the more sizeable uncertainty (largely the result of the more scattered data). It is noteworthy that this procedure reduces the shift of ~0.5 eV observed in the absolute thresholds to one in the relative thresholds of about 0.1 eV. Overall, it appears that the relative threshold energies of these higher order processes can be successfully measured using this approach, although judicious application to processes in which four or more ligands are lost is still called for. At the very least, such measurements can provide more accurate upper limits to these bond energies than are provided by direct measurements of their absolute thresholds.

C. Scaling factors

One disappointing feature of this analysis is the need to introduce the scaling factor f in order to fit the data. The need for this scaling factor is demonstrated in Fig. 3, which shows the results of calculations where no such scaling is included for the $K^+(NH_3)_4$ system. Although the total cross section is reproduced accurately, the branching between the primary dissociation product, $K^+(NH_3)_3$, and the remaining products is not adequately represented. Clearly, too much dissociation is predicted such that scaling the dissociation probability P_{D2} by a factor of about 0.5 is needed (see ratio of σ_0 values in Table III). Indeed, the extent of dissociation is overestimated in all systems examined here. For the primary versus secondary dissociations, the scaling factors gradually increase as the complex gets larger [0.14, 0.42, 0.52, and 0.73, respectively, for $x=2-5$ (Table III)]. For the higher order processes, the scaling factors are 0.23 for $x=3$ and ~0.35 for $x=4$ (Table IV), somewhat smaller than for the secondary processes.

It was checked that these scaling factors were not sensitive to τ_l, the time available for dissociation. Neither did these scaling factors change if the locked-dipole potential was included in determining the position of the loose transition states.

The trends in these scaling factors might indicate that the disposition of energy is less statistical as the complexes get smaller, but it is hard to understand why the model reproduces the dependence on collision energy so accurately if this were the case. It is also possible that even though an octopole ion guide is used to efficiently collect all products,

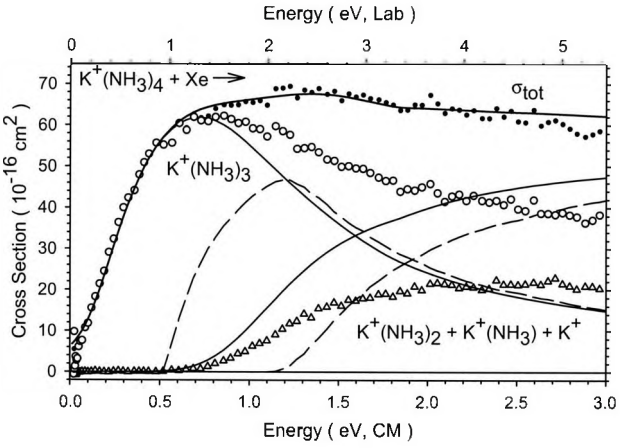

FIG. 3. Zero pressure extrapolated cross sections for collision-induced dissociation of $K^+(NH_3)_4$ with Xe as a function of kinetic energy in the center-of-mass frame (lower x axis) and the laboratory frame (upper x axis) taken from Ref. 56. Solid lines show the fit to the primary and secondary product cross sections using the model of Eq. (8) with no scaling ($f=1$) convoluted over the neutral and ion kinetic and internal energy distributions. Dashed lines show the model cross sections in the absence of experimental kinetic energy broadening for reactions with an internal energy of 0 K.

the higher order reaction products may not be collected as efficiently because there is more kinetic energy release as the extent of dissociation progresses. This would lead to secondary product cross sections that are smaller than predicted, as observed. However, the energy dependence of the total cross sections seems reasonable, such that it seems unlikely that this effect could account for all of the observed differences between experiment and the theoretical prediction. One likely factor that is not accurately included in the statistical model outlined here is rigorous angular momentum conservation. In the treatment above, the most critical component of angular momentum conservation is considered by making sure that the 2D rotational energy of the TS couples with the orbital angular momentum of the primary products. Rotational excitation of the ionic and neutral products is allowed for in a statistical sense, but angular momentum conservation could restrict the range of excitations allowed. It seems plausible that the neglect of such factors could inhibit the dissociation beyond the statistical treatment outlined here. Unfortunately, a rigorous phase space analysis of such sequential dissociations is an especially challenging project. Rather, it is hoped that continued examination of the trends in this empirical scaling parameter as additional studies are conducted will reveal its origins.

IV. CONCLUSIONS

Previously outlined statistical methods for analyzing the experimental results of kinetic energy dependent collision-induced dissociation (CID) experiments[54,55] are extended to situations involving sequential dissociation processes. The present model starts with an empirical threshold function that has been modified to include statistical unimolecular rate theory for the estimation of the lifetime for dissociation. Because most CID studies of interest involve loose transition states, it is appropriate to use statistical assumptions to estimate the disposal of the energy available to the products of the first dissociation, $M^+L_{x-1}+L$. This leads to expressions for the energy distributions in the translational energy of the products, the internal energy in the neutral product L, and the internal energy in the ionic product M^+L_{x-1}. The latter is then used in the calculation of the sequential dissociation probability again using statistical unimolecular rate theory. This model is found to reproduce the energy dependent cross sections for the primary and secondary dissociation channels of $K^+(NH_3)_x$, $x=2-5$,[56] over extended energy and magnitude ranges. Absolute threshold values obtained for the secondary process match those predicted from the sums of the appropriate primary thresholds in all four cases. The model can also be used to obtain reasonable thermodynamic information for higher order dissociations by using information gleaned from the relative thresholds. In addition to the threshold energy for the secondary process, the excellent reproduction of the data and literature thermodynamic information requires a scaling factor (f) for the secondary dissociation probability (P_{D2}). Several possible explanations for this scaling factor are discussed, but continued investigations are needed to quantify its origin.

ACKNOWLEDGMENT

This work is supported by National Science Foundation Grant No. CHE-0451477.

[1] T. O. Tiernan and R. L. C. Wu, Adv. Mass Spectrom. **7A**, 136 (1978).
[2] R. L. C. Wu and T. O. Tiernan, Planet. Space Sci. **7**, 735 (1981).
[3] D. A. Prinslow and P. B. Armentrout, J. Chem. Phys. **94**, 3563 (1991).
[4] E. R. Fisher, B. L. Kickel, and P. B. Armentrout, J. Chem. Phys. **97**, 4859 (1992).
[5] E. R. Fisher, B. L. Kickel, and P. B. Armentrout, J. Phys. Chem. **97**, 10204 (1993).
[6] C. L. Haynes, W. Freysinger, and P. B. Armentrout, Int. J. Mass Spectrom. Ion Process. **149/150**, 267 (1995).
[7] C.-Y. Lin, R. C. Dunbar, C. L. Haynes, P. B. Armentrout, D. S. Tonner, and T. B. McMahon, J. Phys. Chem. **100**, 19659 (1996).
[8] S. T. Graul and R. R. Squires, J. Am. Chem. Soc. **112**, 2517 (1990).
[9] J. A. Paulino and R. R. Squires, J. Am. Chem. Soc. **113**, 5573 (1991).
[10] J. A. Paulino and R. R. Squires, J. Am. Chem. Soc. **113**, 1845 (1991).
[11] R. R. Squires, Int. J. Mass Spectrom. Ion Process. **117**, 565 (1992).
[12] L. S. Sunderlin and R. R. Squires, J. Am. Chem. Soc. **115**, 337 (1993).
[13] T. D. Ranatunga, J. C. Poutsma, R. R. Squires, and H. I. Kenttämaa, Int. J. Mass Spectrom. Ion Process. **128**, L1 (1993).
[14] P. G. Wenthold and R. R. Squires, J. Am. Chem. Soc. **116**, 6401 (1994).
[15] P. G. Wenthold and R. R. Squires, J. Phys. Chem. **99**, 2002 (1995).
[16] T. F. Magnera, D. E. David, and J. Michl, J. Am. Chem. Soc. **111**, 4100 (1989).
[17] T. F. Magnera, D. E. David, D. Stulik, R. G. Orth, H. T. Jonkman, and J. Michl, J. Am. Chem. Soc. **111**, 5036 (1989).
[18] P. J. Marinelli and R. R. Squires, J. Am. Chem. Soc. **111**, 4101 (1989).
[19] L. S. Sunderlin, D. Wang, and R. R. Squires, J. Am. Chem. Soc. **114**, 2788 (1992).
[20] L. S. Sunderlin, D. Wang, and R. R. Squires, J. Am. Chem. Soc. **115**, 12060 (1993).
[21] P. B. Armentrout, Acc. Chem. Res. **28**, 430 (1995).
[22] M. B. More, E. D. Glendening, D. Ray, D. Feller, and P. B. Armentrout, J. Phys. Chem. **100**, 1605 (1996).
[23] D. Ray, D. Feller, M. B. More, E. D. Glendening, and P. B. Armentrout, J. Phys. Chem. **100**, 16116 (1996).
[24] L. Capron, W. Y. Feng, C. Lifshitz, B. L. Tjelta, and P. B. Armentrout, J. Phys. Chem. **100**, 16571 (1996).
[25] M. T. Rodgers and P. B. Armentrout, J. Phys. Chem. A **101**, 2614 (1997).
[26] M. T. Rodgers and P. B. Armentrout, J. Phys. Chem. A **103**, 4955 (1999).
[27] P. B. Armentrout and M. T. Rodgers, J. Phys. Chem. A **104**, 2238 (2000).
[28] M. T. Rodgers and P. B. Armentrout, Mass Spectrom. Rev. **19**, 215 (2000).
[29] M. T. Rodgers and P. B. Armentrout, Acc. Chem. Res. **37**, 989 (2004).
[30] S. G. Anderson, A. T. Blades, J. Klassen, and P. Kebarle, Int. J. Mass Spectrom. Ion Process. **141**, 217 (1995).
[31] J. S. Klassen, S. G. Anderson, A. T. Blades, and P. Kebarle, J. Phys. Chem. **100**, 14218 (1996).
[32] A. Grushow and K. M. Ervin, J. Am. Chem. Soc. **117**, 11612 (1995).
[33] J. R. Stanley, R. Amunugama, and M. T. Rodgers, J. Am. Chem. Soc. **122**, 10969 (2000).
[34] R. Amunugama and M. T. Rodgers, J. Phys. Chem. A **106**, 5529 (2002).
[35] C. Ruan and M. T. Rodgers, J. Am. Chem. Soc. **126**, 14600 (2004).
[36] N. S. Rannulu, R. Amunugama, Z. Yang, and M. T. Rodgers, J. Phys. Chem. A **108**, 6385 (2004).
[37] R. H. Schultz and P. B. Armentrout, Int. J. Mass Spectrom. Ion Process. **107**, 29 (1991).
[38] P. B. Armentrout, D. A. Hales, and L. Lian, in *Advances in Metal and Semiconductor Clusters*, edited by M. A. Duncan (JAI, Greenwich, 1994), Vol. 2, pp. 1–39.
[39] N. F. Dalleska, K. Honma, and P. B. Armentrout, J. Am. Chem. Soc. **115**, 12125 (1993).
[40] S. T. Graul, M. E. Schnute, and R. R. Squires, Int. J. Mass Spectrom. Ion Process. **96**, 181 (1990).
[41] L. S. Sunderlin and R. R. Squires, Chem. Phys. Lett. **212**, 307 (1993).
[42] L. Hanley, J. L. Whitten, and S. L. Anderson, J. Phys. Chem. **92**, 5803 (1988).
[43] M. B. Sowa-Resat, P. A. Hintz, and S. L. Anderson, J. Phys. Chem. **99**, 10736 (1995).
[44] R. H. Schultz, K. C. Crellin, and P. B. Armentrout, J. Am. Chem. Soc. **113**, 8590 (1991).

[45] K. M. Ervin and P. B. Armentrout. J. Chem. Phys. **83.** 166 (1985).
[46] N. F. Dalleska. K. Honma. L. S. Sunderlin. and P. B. Armentrout. J. Am. Chem. Soc. **116.** 3519 (1994).
[47] P. B. Armentrout. in *Advances in Gas Phase Ion Chemistry*. edited by N. G. Adams and L. M. Babcock (JAI Press. Greenwich. 1992). Vol. 1. pp. 83–119.
[48] P. B. Armentrout. J. Am. Soc. Mass Spectrom. **13.** 419 (2002).
[49] R. G. Gilbert and S. C. Smith. *Theory of Unimolecular and Recombination Reactions* (Blackwell Scientific. London. 1990).
[50] T. Baer and W. L. Hase. *Unimolecular Reaction Dynamics: Theory and Experiments* (Oxford University Press. New York. 1996).
[51] K. A. Holbrook. M. J. Pilling. and S. H. Robertson. *Unimolecular Reactions*. 2nd ed. (Wiley. New York. 1996).
[52] S. K. Loh. D. A. Hales. L. Lian. and P. B. Armentrout. J. Chem. Phys. **90.** 5466 (1989).
[53] F. A. Khan. D. E. Clemmer. R. H. Schultz. and P. B. Armentrout. J. Phys. Chem. **97.** 7978 (1993).
[54] M. T. Rodgers. K. M. Ervin. and P. B. Armentrout. J. Chem. Phys. **106.** 4499 (1997).
[55] M. T. Rodgers and P. B. Armentrout. J. Chem. Phys. **109.** 1787 (1998).
[56] C. Iceman and P. B. Armentrout. Int. J. Mass. Spectrom. **222.** 329 (2003).
[57] A. W. Castleman. Jr.. Chem. Phys. Lett. **53.** 560 (1978).
[58] F. Muntean and P. B. Armentrout. J. Chem. Phys. **115.** 1213 (2001).
[59] T. S. Beyer and D. F. Swinehart. Commun. Assoc. Computing Machinery **16.** 379 (1973).
[60] E. V. Waage and B. S. Rabinovitch. Chem. Rev. (Washington. D.C.) **70.** 377 (1970).
[61] V. F. DeTuri and K. M. Ervin. J. Phys. Chem. A **103.** 6911 (1999).
[62] W. J. Chesnavich and M. T. Bowers. in *Gas Phase Ion Chemistry*. edited by M. T. Bowers (Academic. New York. 1979). Vol. 1. pp. 119–151.
[63] J. I. Steinfeld. J. S. Francisco. and W. L. Hase. *Chemical Kinetics and Dynamics* (Prentice Hall. Englewood Cliffs. 1989).